Miniaturized chemical sensor with bio-inspired micropillar working electrode array for lead detection

Citation: Wang, Nan, Elgar Kanhere, Jianmin Miao, and Michael S. Triantafyllou. "Miniaturized Chemical Sensor with Bio-Inspired Micropillar Working Electrode Array for Lead Detection." Sensors and Actuators B: Chemical 233 (October 2016): 249–256.

As Published: http://dx.doi.org/10.1016/j.snb.2016.04.048

Publisher: Elsevier

Persistent URL: http://hdl.handle.net/1721.1/110684

Version: Author's final manuscript: final author's manuscript post peer review, without publisher's formatting or copy editing

Miniaturized chemical sensor with bio-inspired micropillar working electrode array for lead detection

Nan Wang [a], Elgar Kanhere [a], Jianmin Miao [a*], Michael S. Triantafyllou [b, c]

[a] *School of Mechanical and Aerospace Engineering, Nanyang Technological University, 50 Nanyang Avenue, 639798, Singapore*
[b] *Center for Environmental Sensing and Modeling (CENSAM) IRG, Singapore-MIT Alliance for Research and Technology (SMART), 138602, Singapore*
[c] *Department of Mechanical Engineering, Massachusetts Institute of Technology, 77 Massachusetts Avenue, Cambridge, MA 02139, USA*

Keywords: Bio-inspired electrode array, MEMS chemical sensor, Hydrodynamic preconcentration, Anodic stripping voltammetry, Lead detection

Abstract

A disposable, miniaturized and compact microelectromechanical systems (MEMS) chemical sensor incorporated with three-dimensional, free-standing micropillar working electrode array was proposed, fabricated and tested for electrochemical detection of lead ions. Inspiration of designing arch-shaped columnar sensing electrode array originated from the biological imitation of shark's olfactory sensing system, considering shark has developed ultrasensitive olfactory capacity during the evolution processes. The analytical performance of proposed bio-inspired MEMS chemical sensor was comprehensively investigated. Under optimal conditions, high sensitivity of 32 nA/(μg/L) as well as favorable detection limit of 0.2 μg/L was achieved with short deposition time of 30 s. The sensor exhibited linear responses to lead ions in the concentration range from 1 to 130 μg/L with good linearity (correlation coefficient: 0.9994). The collection efficiency towards target ions in the preconcentration step was significantly enhanced by the presence of micropillar electrode array, due to both the enlargement of electrode surface area and the interaction effect between protruding micropillars and moving solution. Proposed MEMS chemical sensor eliminates the involvement of mechanical/forced stirring of testing solution, making it a potential alternative to conventional macro-sized electrochemical sensor for the application of on-site determination of heavy metal contamination.

1. Introduction

Heavy metal contamination poses great detrimental effect on human health as well as aquatic ecosystem due to the non-biodegradable nature, among which lead is treated as one of the

most toxic heavy metals. Excessive intake of lead will induce plenty of neurological, hematological and renal side effects, such as cognitive and behavioral impairment of infants and children [1], restraint of the formation of hemoglobin [2] and chronic kidney dysfunction or hyperuricemia [3]. Immoderate anthropogenic activities, especially discharge of untreated wastewater which usually contains a large quantity of heavy metals, severely deteriorate the quality of different water bodies, e.g. lakes, rivers and streams. These places are considered to be natural reservoirs to supply fresh water to human society and ecosystem. A small area of heavy metal pollution will rapidly sprawl into downstream waters. Hence, continuous monitoring of contamination levels of heavy metal ions at crucial water areas is helpful in quickly identifying the pollution source and minimizing the dissemination issue to a large extent. On-site field measurement of heavy metal pollution requires a compact and portable sensing system which can be easily and quickly operated without complicated accessories. Therefore, development of low-cost, easy-to-use, disposable, miniaturized and sensitive chemical sensors that can be integrated into the sensing system will be highly desirable. Unfortunately, conventional heavy metal detection techniques are not suitable for on-site measurement as they typically rely on laboratory analysis of routinely-collected water samples from a number of locations. Besides, experiments to quantify the concentration of metal ions with analytical techniques such as atomic absorption spectrometry (AAS) [4, 5], inductively coupled plasma atomic emission spectrometry (ICP-AES) [6] and inductively coupled plasma mass spectrometry (ICP-MS) [7, 8], are relatively complicated, time-consuming and require well-trained personnel to operate the equipment. In addition, unpredictable physical, chemical and biological reactions may occur in the samples during prolonged process of transportation and storage, which greatly diminishes the reliability of lab-based testing.

To address the abovementioned concerns, mercury electrodes, including mercury film electrodes [9, 10] and hanging mercury drop electrodes [11, 12], have been conventionally used for the determination of heavy metal ions with stripping voltammetric methods. These electrochemical techniques, especially anodic stripping voltammetry (ASV), have attracted extensive interest from both academic and industrial areas to conduct on-site field evaluation of different heavy metal ions because of the cost-effective instrumentation, simple operation, high sensitivity, high selectivity and portability [13, 14]. However, the toxicity of mercury makes it unsuitable for on-site environmental monitoring in consideration of the adverse health effect brought by the mercury. Bismuth, an environmentally friendly element, provides an alternative electrode material for the application of heavy metal detection in natural

environment due to the attractive electrochemical features, e.g. reproducible stripping behavior, broad linear range and good signal-to-background ratio etc. [15]. The bismuth-based electrodes can be prepared by simultaneously depositing bismuth and target metal ions onto the working electrode during the deposition process [14, 16]. Advantage of such approach reveals on the fact that target heavy metal ions together with bismuth ions are able to form a multicomponent alloy [15], which highly accelerates the preconcentration of metal ions on the electrode surface, a crucial step of electroanalytical stripping analysis to enhance the sensitivity of heavy metal quantification. There are also some other effective methods focusing on augmentation of sensitivity for heavy metal detection, e.g. covalent attachment of aryl radical onto the surface of glassy carbon spheres [17] as well as the use of bifunctional periodic mesoporous organosilica [13], siloxane-crown ether polyamide copolymer [18], thymine-thymine mismatch-based oligonucleotide molecular beacon [19], and metal-ion mediated gold nanoparticle-based assembly [20] to modify or functionalize the surface of the electrode.

Recently, the employment of screen-printed electrodes (SPEs) coupled with electrochemical stripping voltammetry gained widespread attention regarding field measurement of heavy metals, owing to the possibility of mass production of SPEs and attractive merits of stripping analysis, such as low cost, favorable operation and high sensitivity. Research pertaining to both commercially-available [21] and lab-built [22] SPEs has been widely reported due to the simple processes involved in the preparation of planar SPEs. On the other hand, modifications of the working electrode surface of SPEs have also been extensively investigated by using variety of materials, such as electrochemically reduced bismuth oxide [23], 4-carboxy-phenyl diazonium [24] and graphene/ionic liquid composite [25]. Although SPEs have the potential to replace conventional macro-sized electrodes, effectiveness of SPEs to detect low concentration samples highly depends on the mass transport efficiency of metal ions towards the electrode surface. In general, vigorous stirring of testing solution [26-28] is involved in the course of electrochemical measurement to ensure adequate metal ions can be transported to the vicinity of sensing electrode. Sensitivity of SPEs would be dramatically diminished if stirring cannot be provided. The usage of mechanical intervention (stirring accessories) will complicate the packaging of whole chemical sensor, compromising the device operability, portability as well as miniaturization for on-site application.

In an attempt to circumvent this problem, a miniaturized, portable, compact, MEMS-based chemical sensor is proposed by deriving the inspiration from shark’s olfactory sensing

system. It is incontrovertible that during the evolution process, survival instinct impels various creatures to be equipped with incredibly sensitive sensors [29-32]. As for odorant sensing in the water, shark is one of the most reputed aquatic animals, since their sensing organs are highly responsible for perceiving and analyzing odorant information to initiate food searching, and to mediate the reproduction behavior [33]. As shown in Figure 1A, the olfactory organs of pelagic sharks, e.g. great white shark, lemon shark and tiger shark etc., are situated at the ventral side of the head and are completely isolated from the mouth, suggesting exclusive function for odorant detection instead of assisting in respiration [34]. Inside the olfactory cavity, a large number of olfactory lamellae (Figure 1B) aggregate a rosette layout [35] to form internal gap system between opposite-facing lamellae for water circulation. Such structure will significantly increase the chances of odorant molecules to be captured by olfactory sensing system. The olfactory sensors of sharks, also known as olfactory receptor cells, are embedded beneath a layer of pseudostratified, columnar sensory epithelium (Figure 1C), which covers more surface area of each olfactory lamella than the nonsensory epithelium [36]. The morphological distribution of the olfactory receptor cells enlarges the total sensing area that is exposed to surrounding water, enabling sharks to develop highly sensitive olfactory sensing in water.

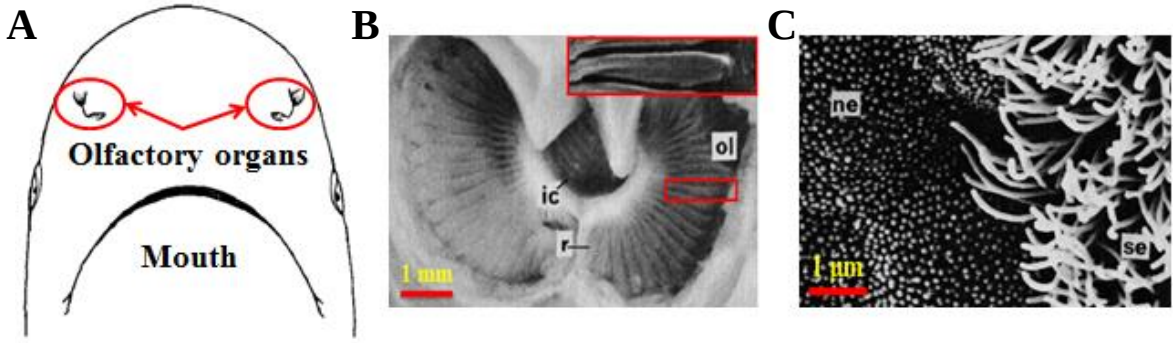

Figure 1. (A) Ventral view of lemon shark to show the location of olfactory organs [20]. (B) Cross-sectional SEM image [20] of one olfactory organ to show abundant layers of olfactory lamellae (ol), where ‘ic’, inlet chamber; ‘r’, raphe. Inset depicts enlarged view of one piece of lamella, which is enclosed in red rectangular box. (C) SEM image [20] with high magnification to show bundles of olfactory receptor cells on the sensory epithelium (se), scattered on the side wall of one piece of lamella, where ‘ne’, nonsensory epithelium. Modified with the permission of the NRC Research Press.

Inspired by the hydrodynamically efficient and fascinating structure of shark’s olfactory sensing system, a MEMS chemical sensor with bio-inspired free-standing micropillar working electrode array is proposed in order to develop an artificial counterpart of the shark’s olfactory sensors. As shown in Figure 2A, proposed sensor consists of a top microfluidic

channel with total volume of 1.8 mm^3 and a bottom sensor base with three miniaturized, semi-circle, on-chip base electrodes, i.e. reference electrode, working electrode and counter electrode. An arch-shaped electrode array comprising 24 micropillars with diameter of 0.1 mm and height of 0.12 mm is incorporated onto the base working electrode to imitate the morphological arrangement of shark's olfactory sensing system. Such a three-dimensional design of pillar electrodes enlarges the sensing area of chemical sensor while keeping the device footprint to a minimum. When the testing solution is injected into the chamber of microfluidic channel through inlet, it will be immediately guided into those subchannels constructed by adjacent pillar electrodes, efficaciously improving the collection efficiency of target ions dissolved in the solution. This bio-inspired configuration highly resembles the gap system of shark's olfactory system (Figure 2B) to facilitate the dispersion of water, thereby boosting the sensitivity of odorant detection [37]. Dimensions of microfluidic channel as well as miniaturized on-chip electrodes together with arch-shaped micropillar electrode array are depicted in Figure 3A and 3B.

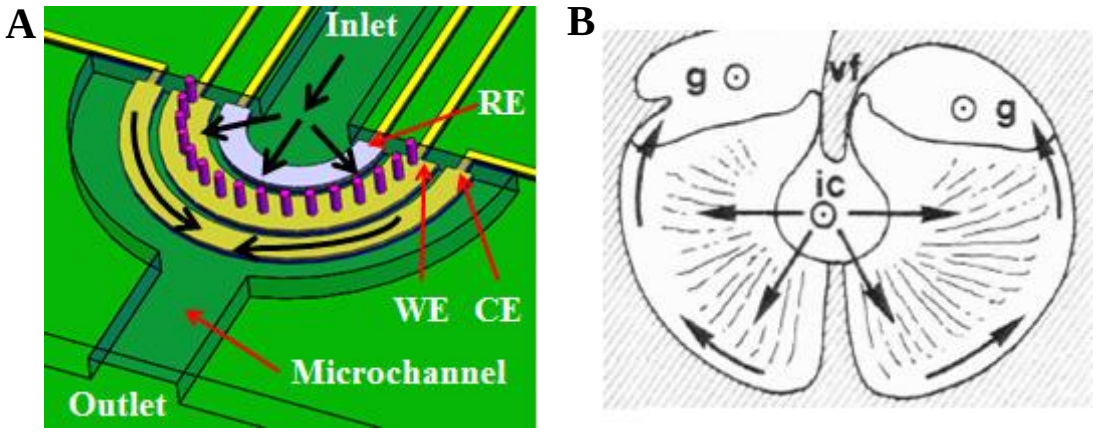

Figure 2. (A) Schematic diagram of bio-inspired MEMS chemical sensor to illustrate the flow path (black arrows) of testing solution passing through the microfluidic channel, where 'RE', reference electrode; 'WE', working electrode; 'CE', counter electrode. (B) Schematic drawing of the gap system of mud shark [21] to show water dispersion (black arrows) through the olfactory organ, where 'ic', inlet chamber; 'vf', valve flap; 'g', gallery. Reprinted with the permission of the John Wiley and Sons.

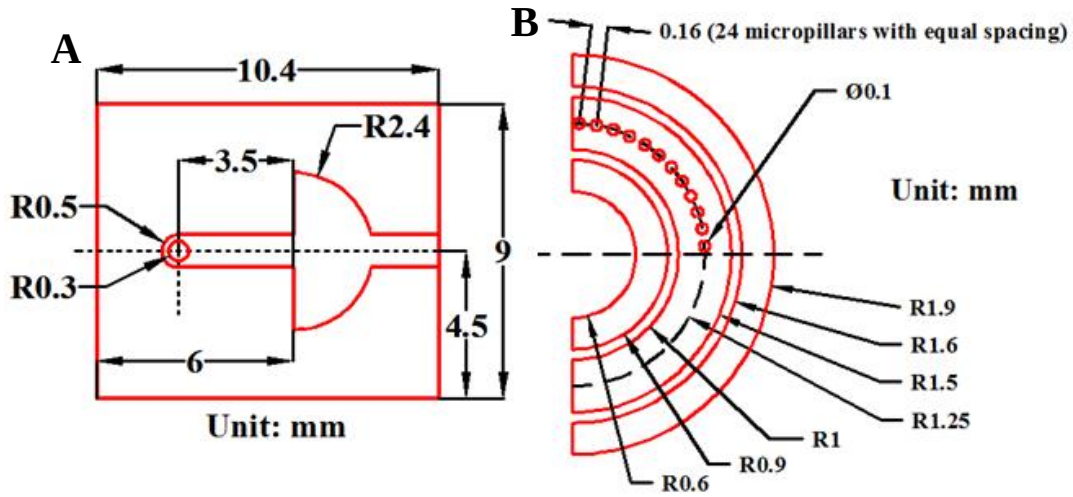

Figure 3. Dimensions of (A) microfluidic channel and (B) miniaturized, on-chip electrodes together with arch-shaped micropillar electrode array (only half of 24 micropillars are shown in the drawing to improve the clarity).

2. Experimental

2.1 Sensor fabrication

Proposed bio-inspired MEMS chemical sensor consists of different structural layers as shown in Figure 4. Fabrication of the chemical sensor was commenced by depositing 1 µm silicon dioxide (SiO_2) insulation layer on the 500 µm, P-type silicon (Si) substrate. After patterning with positive photoresist, a 300 nm layer of gold (Au) was sputtered to provide the electrical connection for each electrode, under which another layer of 100 nm chromium (Cr) was introduced for promoting the adhesion with underlying SiO_2 layer. Subsequently, lift-off processes were performed to define the position of base working electrode (600 nm Au) as well as base reference electrode (500 nm silver (Ag) combined with silver chloride (AgCl)). Thereafter, a layer of 120 µm SU-8 negative photoresist was spin-coated and then exposed to the UV light to shape the core of micropillar electrodes. A thin film of 200 nm Au was coated on both top surface and side surface of each pillar to make the micropillar working electrode array to be electrically connected with the base electrode. Finally, the fabricated sensor was covered by a polydimethylsiloxane (PDMS) microfluidic channel, producing a bio-inspired reaction chamber together with the micropillar electrode array. Detailed fabrication process of sensor base with micropillar electrode array (refer to Figure S1 in the supplementary material) and the one of PDMS microfluidic channel (refer to Figure S2 in the supplementary material) are described in the supplementary material. The photograph of proposed MEMS chemical sensor with three-electrode configuration after fabrication is shown in Figure 5A

and the scanning electron microscope (SEM) image of micropillar working electrode array is shown in Figure 5B.

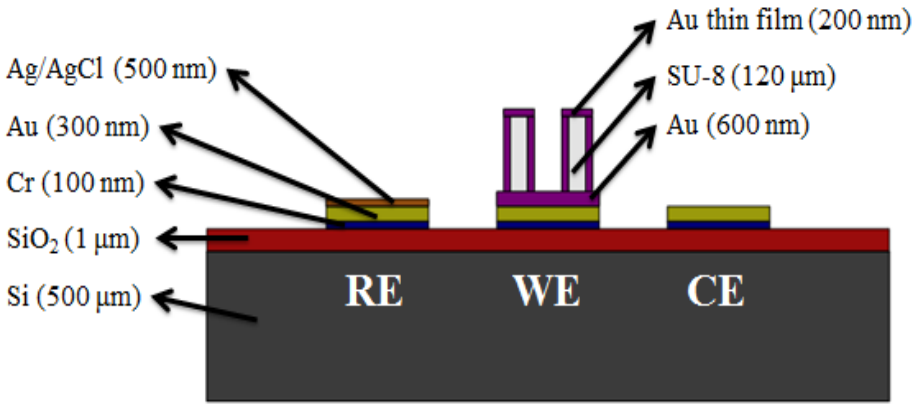

Figure 4. Schematic side view of proposed bio-inspired MEMS chemical sensor to show different structural layers.

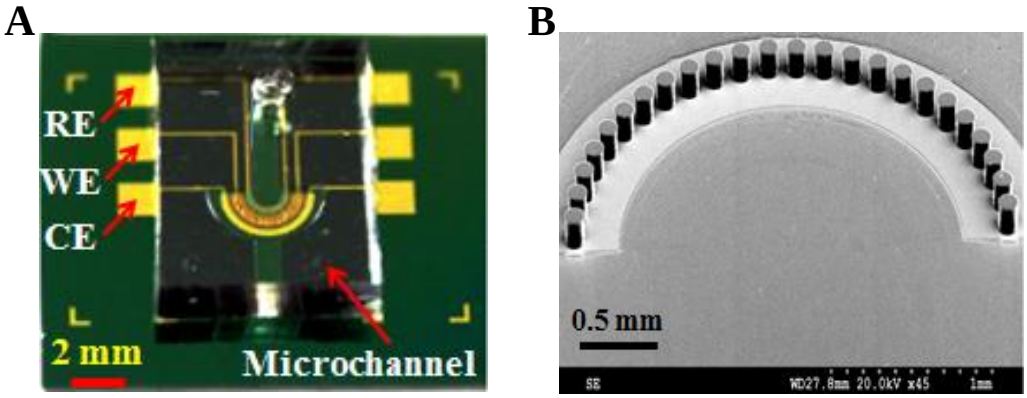

Figure 5. (A) Photograph of proposed bio-inspired MEMS chemical sensor after fabrication, where 'RE', reference electrode; 'WE', working electrode; 'CE', counter electrode. (B) SEM image of micropillar working electrode array.

2.2 Chemicals and reagents

All the chemicals used in this study were of analytical grade and purchased from Sigma-Aldrich (Singapore) unless stated otherwise. Deionized water (18.2 MΩ·cm) collected from a Milli-Q system (Millipore, Singapore) was used throughout for solution preparation. A solution containing 2 mM potassium hexacyanoferrate ($K_3[Fe(CN)_6]$) and 0.2 M potassium chloride (KCl) was prepared for the experiment of cyclic voltammetry by dissolving appropriate amount of power into water. Bismuth standard stock solution (1000 mg/L) was obtained from Merck (Singapore). Diluted lead solution was prepared from atomic absorption standard solution (1000 mg/L). 0.1 M acetate buffer (pH 4.6) was used as the supporting electrolyte for the experiment of ASV.

2.3 Apparatus

All electrochemical experiments were carried out using a CHI 600C electrochemical workstation (CH Instruments, USA). Commercial Au working electrode (3 mm diameter), Ag/AgCl (3 M NaCl) reference electrode and platinum (Pt) counter electrode purchased from Alpha Analytical (Singapore) were used in the cyclic voltammetry experiment for comparison purpose. A high precision auto-dispenser system supplied by Atome Sciences (Singapore) was employed to precisely control the dispensing of testing solution into the PDMS microfluidic channel.

2.4 Measurement procedure

Cyclic voltammetry was performed by immersing the commercial Au working electrode/ fabricated micropillar working electrode array together with commercial Ag/AgCl reference electrode and commercial Pt counter electrode into the solution of 2 mM $K_3[Fe(CN)_6]$ and 0.2 M KCl as supporting electrolyte. The voltammetric investigation was initiated with an initial potential and final potential of 0.6 V, switching potential of -0.2 V, and scan rate of 50 mV/s. The potential measured in this experiment was with respect to commercial Ag/AgCl reference electrode, while potential of remaining experiments was registered versus fabricated on-chip Ag/AgCl reference electrode. The electrochemical analysis of lead ions with proposed bio-inspired MEMS chemical sensor was implemented by simultaneous accumulation of 300 µg/L bismuth and different concentrations of lead onto the working electrode. Deposition step was carried out by continuously injecting testing solution into the PDMS microchannel with a potential of -0.8 V (after optimization) being applied to the working electrode for 30 s (after optimization). After a 5 s equilibration time, the voltammograms were recorded from -0.8 to 0 V under quiescent condition by square wave anodic stripping voltammetry (SWASV) with frequency of 50 Hz, amplitude of 50 mV and step potential of 5 mV. A conditioning potential of 0 V for 120 s with testing solution being replenished was provided to the working electrode after each measurement in order to remove the residual metal ions. All experiments were performed at room temperature and all solutions were used without prior deaeration.

3. Results and discussion

3.1 Characterization of micropillar working electrode array

With the intent of verifying the presence of Au thin film coated on the micropillar electrodes, energy dispersive spectroscopy (EDS) analysis was conducted to inspect the surface properties of individual micropillar. EDS spectrums, which can aid in revealing elemental constitution of sample surface, are shown in Figure 6A and 6B, corresponding to the top surface and side surface of the micropillar electrode. It is apparent that the micropillar was conformally covered by Au thin film, thereby functioning as a three-dimensional working electrode. Carbon (C) and oxygen (O) traces detected in the spectrum could be possibly due to the strong penetration of high-energy charged particles into the core of micropillar, which was made by SU-8 photoresist - a polymer mainly comprising the element of C and O. Besides, the existence of C and O could also be attributed to any unexpected adulteration of impurities during the experiment. After performing the EDS spectrum analysis, the electrical connection between each micropillar electrode and bottom contact pad was carefully checked under high precision probe station (refer to Figure S3 in the supplementary material) to ensure all of them will be able to serve the function of three-dimensional working electrode. Although the sputtering of Au thin film was confirmed by EDS spectrum analysis, total surface coverage of Au onto the micropillar electrodes was still unknown. To address this concern, cyclic voltammetry in the solution of 2 mM $K_3[Fe(CN)_6]$ with 0.2 M KCl as supporting electrolyte was subsequently conducted to evaluate the surface area of MEMS chemical sensor. For the fabricated sensor, undistorted reduction peak and oxidation peak were observed in comparison with commercial electrode, indicating the capability of proposed MEMS chemical sensor being able to accurately register redox reaction in the vicinity of micropillar working electrode array.

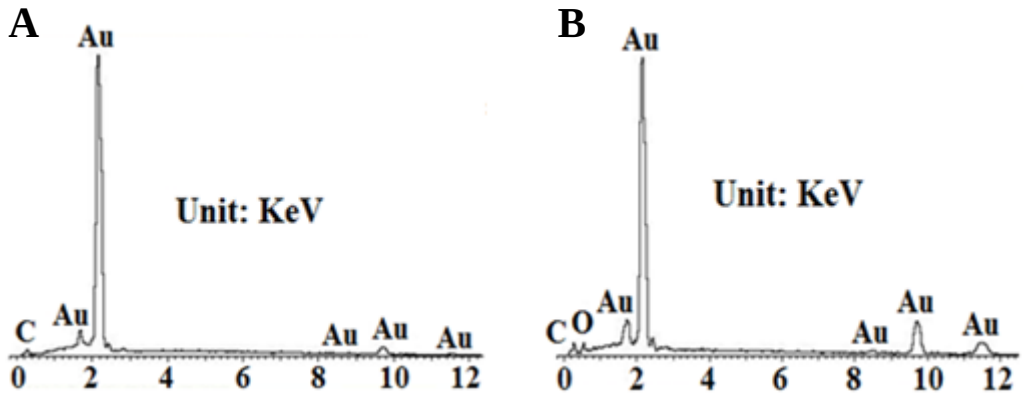

Figure 6. EDS analysis of one micropillar electrode to show elemental constitution of (A) top surface and (B) side surface in the unit of kilo-electronvolt (KeV).

Considering the fact that cyclic voltammetry was operated in the unstirred testing solution, hydrodynamic convection effect had no contribution for the transport of electroactive materials to the working electrode surface. Moreover, migration effect, that is the movement of charged particles along electrical field, could also be neglected given the situation that concentration of supporting electrolyte (0.2 M KCl) was around 100 times higher than the one of electroactive materials (2 mM $K_3[Fe(CN)_6]$). Therefore, electroactive species dissolved in the testing solution would only be transported to the electrode-solution interface by diffusion effect. Under such condition, peak current of cyclic voltammetric experiment can be derived from Randles–Sevcik equation [38] (refer to Section 4 in the supplementary material). By comparing the ratio of peak current, surface area of the sensor's working electrode can be calculated given commercial electrode has about 7.07 mm^2 surface area (calculated based on the diameter of commercial electrode, which is 3 mm). According to the data obtained from cyclic voltammetry (refer to Figure S4, S5, S6 and S7 in the supplementary material), the average value of Au coverage on the sensor without and with micropillar working electrode array is 2.33 ± 0.02 and 3.04 ± 0.03 mm^2, respectively. Theoretical surface area of 24 micropillars together with the bottom base electrode is around 2.87 mm^2 (calculated based on the electrode dimensions, refer to Figure S8 in the supplementary material), demonstrating the micropillar electrode array was completely coated by Au thin film. The extra surface area determined from experimental result is reasonable since the micropillars were fabricated by shining UV light from the top of SU-8 photoresist layer. Diffraction of UV light through the photomask during the exposure step will result in a slight enlargement of the diameter of each micropillar [39-41].

3.2 Optimization of deposition potential and deposition time

For preliminary investigation of the electrochemical behavior of proposed MEMS chemical sensor with micropillar electrode array, cyclic voltammetry was performed in the solutions of 0.1 M acetate buffer without and with 10 mg/L lead and 50 mg/L bismuth ions. As shown in Figure 7, the sensor showed clear reduction and oxidation peaks when lead and bismuth were present in the solution, demonstrating high possibility to use proposed sensor for lead detection. In order to optimize the performance of the sensor, two important parameters pertaining to the preconcentration process, i.e. deposition potential and deposition time, were carefully evaluated. The effect of deposition potential on the stripping peak current of lead for the sensor with micropillar working electrode array was investigated from -0.5 to -1.1 V by keeping deposition time as well as flow rate unchanged (refer to Figure S9 in the

supplementary material). The magnitude of peak current was initially increased in the period where deposition potential became more negative, owing to the fact that higher energy was supplied to induce more metal ions to participate in the process of electrochemical reduction. The highest peak current was observed at -0.8 V deposition potential, after which stripping peak began to drop gradually on account of the enhanced evolution of hydrogen. A very similar trend was found by Honeychurch et al. [42], when a microband carbon SPE was used to evaluate the impact of deposition potential. The study conducted by Wang et al. [25] with a disposable ionic liquid SPE modified by electrochemical reduction of graphene oxide also confirmed this tendency.

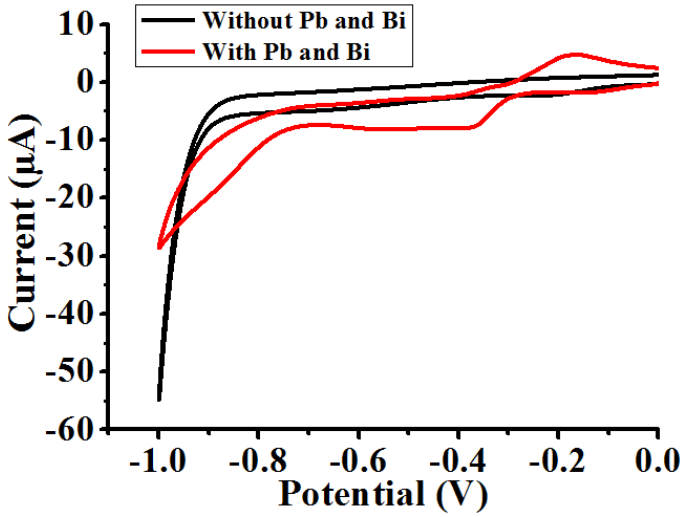

Figure 7. Cyclic voltammograms of proposed MEMS chemical sensor with micropillar electrode array in 0.1 M acetate buffer without (in black) and with (in red) 10 mg/L lead and 50 mg/L bismuth ions. Initial and final potential: 0 V; switching potential: -1.0 V; scan rate: 50 mV/s. Potentials were measured with respect to fabricated on-chip Ag/AgCl reference electrode.

As for the deposition time, its influence on the stripping peak current of lead was analyzed between 10 and 70 s (refer to Figure S10 in the supplementary material). In the beginning, stripping current greatly increased until a relative plateau level was attained, and then started to decrease slowly. The elevation of peak current can be explained by the reason that more metal ions were dispensed into the microfluidic channel, which brought more electroactive materials to be transported into the vicinity of micropillar working electrode array. However, prolonged deposition time could make the electrode surface to be quickly saturated, leading to the stagnation and/or decline of peak current. The phenomenon was also discovered by Rico et al. [21] using a carbon SPE and Figueiredo-Filho et al. [43] using a mini-sensor modified with bismuth film. In order to avoid the saturation of working electrode,

especially at high concentration, the deposition time was selected to be 30 s, to keep the best compromise between measurement time and sensitivity.

3.3 Evaluation of the effect of flow rate

The impact of dispensing flow rate on the lead peak current was determined from 0.15 to 0.64 μL/s with unvaried deposition potential and deposition time. As shown in Figure 8A, peak current of MEMS chemical sensor with micropillar electrode array significantly became higher when the testing solution was fed at higher flow rate. On the contrary, for the sensor without micropillar electrode array, the magnitude of stripping current tended to be lower with increased flow rate. If the difference of peak current is only caused by the disparity of surface area, based on the results from cyclic voltammetry (refer to Section 3.1), stripping peak for the sensor with micropillar electrode array should be approximately 30% higher than the stripping peak for the sensor without micropillar electrode array. However, Figure 8B shows that percentage increase of peak current between the sensor with and without micropillar electrode array already approaches to 74% even at the lowest flow rate. Furthermore, peak current ratio continues to accumulate when flow rate is augmented.

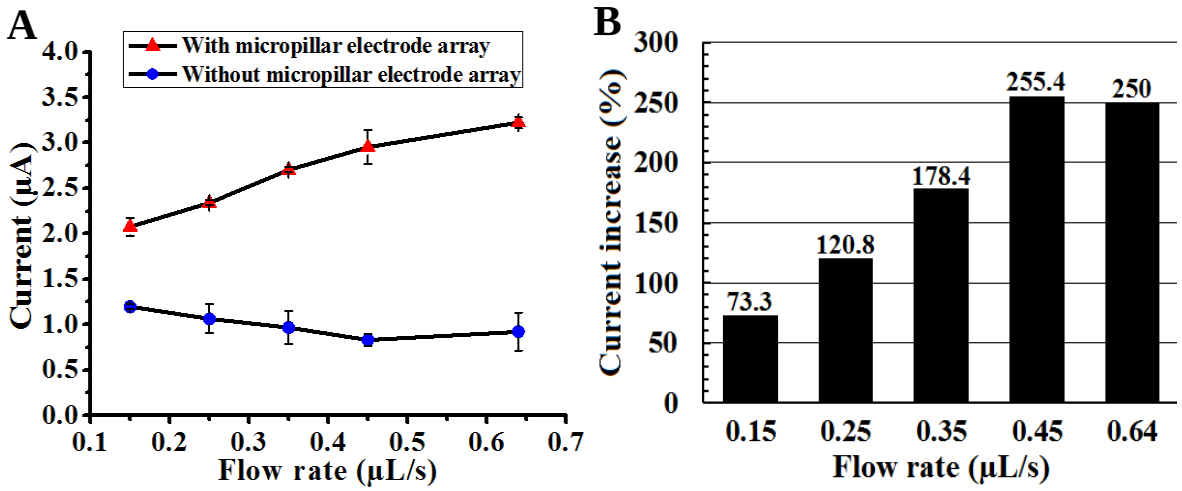

Figure 8. (A) Influence of flow rate on the stripping peak current of 30 μg/L lead solution in 0.1 M acetate buffer using MEMS chemical sensor with and without micropillar electrode array. (B) Percentage increase of peak current between MEMS chemical sensor with and without micropillar electrode array. Deposition potential: -0.8 V; deposition time: 30 s. Potentials were measured with respect to fabricated on-chip Ag/AgCl reference electrode. Data are presented with the mean of three replicates.

Explanation of such interesting observation can be elucidated by the enhancement of collection efficiency of metal ions during the preconcentration step, whereby flat working

electrode will be inevitably concealed inside the boundary layer generated by moving solution, resulting in a mass of sample ions being wasted. However, micropillar electrodes are able to extend from the flow stagnation region owing to the vertical dimension of sensing surface, which greatly magnifies the amount of metal ions absorbed to the working electrode over equal periods of deposition time. Another remarkable contribution of micropillar electrode array embodies at the aspect that an artificial gap system is automatically formed among adjacent pillars, which will assist in convective expansion of testing solution, thereby bringing more target ions to be adequately in contact with working electrode surface. In addition, arch-shape distribution of micropillar electrode array takes the advantage of fluid dynamics, in which the parabolic shape of the three-dimensional electrode array follows the velocity profile of moving flow developed along the horizontal direction of the microfluidic channel, making the sensing surface of all micropillar electrodes to participate in the process of collecting metal ions in the testing solution. Conversely, the majority of testing solution will only pass through the middle section of flat working electrode for the sensor without micropillar electrode array, leading to prominent diminishment of ion collection efficiency.

3.4 Calibration of the proposed MEMS chemical sensor

Calibration of proposed MEMS chemical sensor with micropillar electrode array regarding lead metal ion measurement was conducted by specifying the flow rate of 0.35 μL/s as optimal value in consideration of saturation effect. After seeking out these favorable parameters, a series of SWASV experiments with increasing concentrations of lead ions were recorded. Stripping voltammograms with well-defined, undistorted peaks are depicted in Figure 9A and the corresponding calibration curve is illustrated in Figure 9B. The sensor displayed linear responses towards lead ions in the concentration range from 1 to 130 μg/L. In addition, high analytical sensitivity of 32 nA/(μg/L) and good linearity (R^2=0.9994) were also observed. The limit of detection (LOD) calculated by taking signal-to-noise ratio of 3, reached to 0.2 μg/L with short deposition time of 30 s.

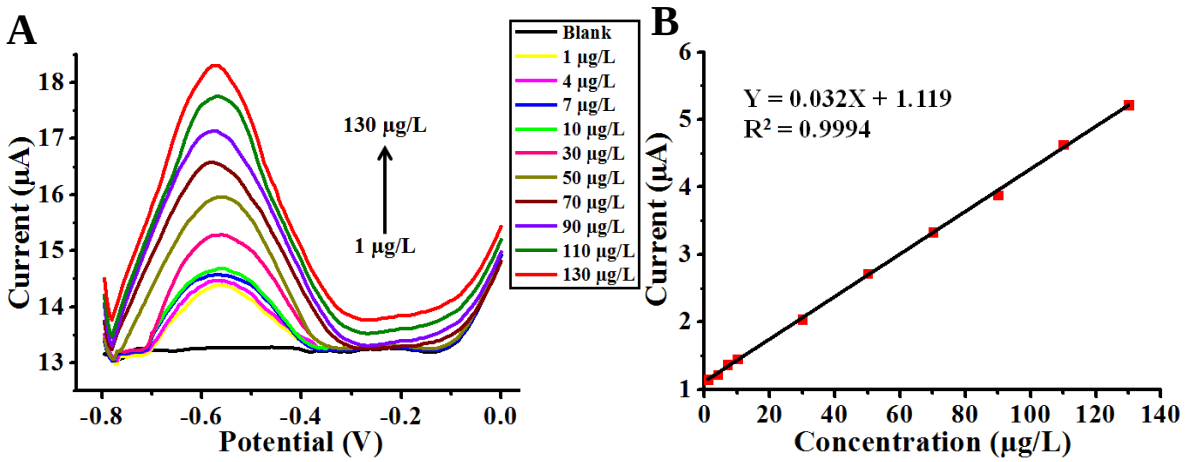

Figure 9. (A) Stripping voltammograms for increasing concentrations of lead ions from 1 to 130 µg/L on proposed MEMS chemical sensor with micropillar electrode array. (B) Calibration curve of stripping peak current versus lead concentration. Deposition potential: -0.8 V; deposition time: 30 s; flow rate: 0.35 µL/s. Potentials were measured with respect to fabricated on-chip Ag/AgCl reference electrode.

4. Conclusions

In this study, a miniaturized MEMS chemical sensor was designed, fabricated, tested and optimized for the determination of lead metal ions by integrating a bio-inspired micropillar working electrode array with a compact microfluidic channel. The idea of incorporating bio-mimicking and bio-inspiration concept into the design of chemical sensor enabled an innovative attempt to develop three-dimensional sensing electrodes. Experimental evaluation showed that favorable analytical sensitivity of 32 nA/(µg/L) as well as limit of detection of 0.2 µg/L was achieved without complicated setup and excessive external involvement in comparison with other SPE/solid-state chemical sensors. It can be noticed that, without the employment of forced mechanical perturbation/stirring to the testing solution, proposed bio-inspired MEMS chemical sensor manifests promising application in terms of on-site, fast and simple detection of lead pollution. However, for real-life environmental monitoring of the lead contamination, it is highly necessary to carry out a comprehensive analysis of the sensor behavior in terms of interference effects with other prevalent metal ions in the water samples, matrix effects induced by possible organic matters or pollutants (e.g. detergents, insecticides, petroleum hydrocarbons and pharmaceuticals etc.) and the influences caused by certain properties (e.g. salinity, acidity, alkalinity and hardness etc.) of the water samples.

Corresponding Author

*Email: MJMMIAO@ntu.edu.sg

Acknowledgements

This research was supported by the Ministry of Education Singapore and the National Research Foundation Singapore through the Singapore MIT Alliance for Research and Technology's Center for Environmental Sensing and Modeling interdisciplinary research program.

References

[1] R.A. Goyer, Lead toxicity: current concerns, Environ. Health Perspect. 100 (1993) 177-187.
[2] R.M. Tripathi, R. Raghunath, S. Mahapatra, S. Sadasivan, Blood lead and its effect on Cd, Cu, Zn, Fe and hemoglobin levels of children, Sci. Total Environ. 277 (2001) 161-168.
[3] P.A. Marsden, Increased body lead burden - cause or consequence of chronic renal insufficiency?, New Engl. J. Med. 348 (2003) 345-347.
[4] I. Lopez-Garcia, Y. Vicente-Martinez, M. Hernandez-Cordoba, Determination of cadmium and lead in edible oils by electrothermal atomic absorption spectrometry after reverse dispersive liquid-liquid microextraction, Talanta 124 (2014) 106-110.
[5] A.V. Zmozinski, L.D. Passos, I.C.F. Damin, M.A.B. Espirito Santo, M.G.R. Vale, M.M. Silva, Determination of cadmium and lead in fresh fish samples by direct sampling electrothermal atomic absorption spectrometry, Anal. Methods 5 (2013) 6416-6424.
[6] M. Uemoto, M. Nagaoka, H. Fujinuma, Interlaboratory testing for the determination of trace amounts of tin and lead in magnesium and magnesium alloys by inductively coupled plasma atomic emission spectrometry, Anal. Sci. 25 (2009) 717-721.
[7] A. Sorbo, A.C. Turco, M. Di Gregorio, L. Ciaralli, Development and validation of an analytical method for the determination of arsenic, cadmium and lead content in powdered infant formula by means of quadrupole inductively coupled plasma mass spectrometry, Food Control 44 (2014) 159-165.
[8] V. Yilmaz, Z. Arslan, L. Rose, Determination of lead by hydride generation inductively coupled plasma mass spectrometry (HG-ICP-MS): On-line generation of plumbane using potassium hexacyanomanganate(III), Anal. Chim. Acta 761 (2013) 18-26.
[9] E. Fischer, C.M.G. van den Berg, Anodic stripping voltammetry of lead and cadmium using a mercury film electrode and thiocyanate, Anal. Chim. Acta 385 (1999) 273-280.
[10] M.F. de Oliveira, A.A. Saczk, L.L. Okumura, A.P. Fernandes, M. de Moraes, N.R. Stradiotto, Simultaneous determination of zinc, copper, lead, and cadmium in fuel ethanol by anodic stripping voltammetry using a glassy carbon-mercury-film electrode, Anal. Bioanal. Chem. 380 (2004) 135-140.
[11] C. Fernandez-Bobes, M.T. Fernandez-Abedul, A. Costa-Garcia, Anodic stripping of heavy metals using a hanging mercury drop electrode in a flow system, Electroanalysis 10 (1998) 701-706.

[12] M.A. Ferreira, A.A. Barros, Determination of As(III) and arsenic(V) in natural waters by cathodic stripping voltammetry at a hanging mercury drop electrode, Anal. Chim. Acta 459 (2002) 151-159.
[13] S. Morante-Zarcero, D. Perez-Quintanilla, I. Sierra, A disposable electrochemical sensor based on bifunctional periodic mesoporous organosilica for the determination of lead in drinking waters, J. Solid State Electrochem. 19 (2015) 2117-2127.
[14] S. Intarakamhang, W. Schuhmann, A. Schulte, Robotic heavy metal anodic stripping voltammetry: Ease and efficacy for trace lead and cadmium electroanalysis, J. Solid State Electrochem. 17 (2013) 1535-1542.
[15] J. Wang, Stripping analysis at bismuth electrodes: A review, Electroanalysis 17 (2005) 1341-1346.
[16] L. Pinto, S.G. Lemos, Comparison of different PLS algorithms for simultaneous determination of Cd(II), Cu(II), Pb(II), and Zn(II) by anodic stripping voltammetry at bismuth film electrode, Electroanalysis 26 (2014) 299-305.
[17] G.K. Raghu, S. Sampath, M. Pandurangappa, Chemically functionalized glassy carbon spheres: a new covalent bulk modified composite electrode for the simultaneous determination of lead and cadmium, J. Solid State Electrochem. 16 (2012) 1953-1963.
[18] I.M. Simionca, A. Arvinte, R. Ardeleanu, M. Pinteala, Siloxane-crown ether polyamide based electrode for electrochemical determination of lead(II) in aqueous solution, Electroanalysis 24 (2012) 1995-2004.
[19] M. Stobiecka, A.A. Molinero, A. Chalupa, M. Hepel, Mercury/homocysteine ligation-induced ON/OFF-switching of a T-T mismatch-based oligonucleotide molecular beacon, Anal. Chem. 84 (2012) 4970-4978.
[20] M. Hepel, D. Blake, M. McCabe, M. Stobiecka, K. Coopersmith, Assembly of gold nanoparticles induced by metal ions, in: M. Hepel, C.J. Zhong (Eds.), Functional Nanoparticles for Bioanalysis, Nanomedicine and Bioelectronic Devices, American Chemical Society, Washington, DC, 2012, pp. 207-240.
[21] M.A.G. Rico, M. Olivares-Marin, E. Pinilla Gil, Modification of carbon screen-printed electrodes by adsorption of chemically synthesized Bi nanoparticles for the voltammetric stripping detection of Zn(II), Cd(II) and Pb(II), Talanta 80 (2009) 631-635.
[22] S. Laschi, I. Palchetti, M. Mascini, Gold-based screen-printed sensor for detection of trace lead, Sens. Actuators B 114 (2006) 460-465.
[23] G.H. Hwang, W.K. Han, J.S. Park, S.G. Kang, An electrochemical sensor based on the reduction of screen-printed bismuth oxide for the determination of trace lead and cadmium, Sens. Actuators B 135 (2008) 309-316.
[24] S. Bouden, A. Chausse, S. Dorbes, O.E. Tall, N. Bellakhal, M. Dachraoui, C. Vautrin-Ul, Trace lead analysis based on carbon-screen-printed-electrodes modified via 4-carboxy-phenyl diazonium salt electroreduction, Talanta 106 (2013) 414-421.
[25] Z.Q. Wang, H. Wang, Z.H. Zhang, G. Liu, Electrochemical determination of lead and cadmium in rice by a disposable bismuth/electrochemically reduced graphene/ionic liquid composite modified screen-printed electrode, Sens. Actuators B 199 (2014) 7-14.
[26] V. Sosa, C. Barcelo, N. Serrano, C. Arino, J.M. Diaz-Cruz, M. Esteban, Antimony film screen-printed carbon electrode for stripping analysis of Cd(II), Pb(II), and Cu(II) in natural samples, Anal. Chim. Acta 855 (2015) 34-40.
[27] S. Cinti, S. Politi, D. Moscone, G. Palleschi, F. Arduini, Stripping analysis of As(III) by means of screen-printed electrodes modified with gold nanoparticles and carbon black nanocomposite, Electroanalysis 26 (2014) 931-939.
[28] C. Chen, X.H. Niu, Y. Chai, H.L. Zhao, M.B. Lan, Y.G. Zhu, G. Wei, Determination of lead(II) using screen-printed bismuth-antimony film electrode, Electroanalysis 25 (2013) 1446-1452.

[29] M.S. Triantafyllou, G.D. Weymouth, J.M. Miao, Biomimetic survival hydrodynamics and flow sensing, Annu. Rev. Fluid Mech. 48 (2016) 1-24.
[30] A.G.P. Kottapalli, M. Bora, M. Asadnia, J.M. Miao, S.S. Venkatraman, M. Triantafyllou, Nanofibril scaffold assisted MEMS artificial hydrogel neuromasts for enhanced sensitivity flow sensing, Sci. Rep. 6 (2016) 19336.
[31] M. Asadnia, A.G.P. Kottapalli, R. Haghighi, A. Cloitre, P.V. y Alvarado, J.M. Miao, M. Triantafyllou, MEMS sensors for assessing flow-related control of an underwater biomimetic robotic stingray, Bioinspir. Biomim. 10 (2015) 036008.
[32] H.R. Beem, M.S. Triantafyllou, Wake-induced 'slaloming' response explains exquisite sensitivity of seal whisker-like sensors, J. Fluid Mech. 783 (2015) 306-322.
[33] E.H. Hamdani, K.B. Doving, The functional organization of the fish olfactory system, Prog. Neurobiol. 82 (2007) 80-86.
[34] L.L. Timm, F.E. Fish, A comparative morphological study of head shape and olfactory cavities of sharks inhabiting benthic and coastal/pelagic environments, J. Exp. Mar. Biol. Ecol. 414 (2012) 75-84.
[35] V. Schluessel, M.B. Bennett, H. Bleckmann, S. Blomberg, S.P. Collin, Morphometric and ultrastructural comparison of the olfactory system in elasmobranchs: The significance of structure-function relationships based on phylogeny and ecology, J. Morphol. 269 (2008) 1365-1386.
[36] E. Zeiske, B. Theisen, S.H. Gruber, Functional morphology of the olfactory organ of two carcharhinid shark species, Can. J. Zool. 65 (1987) 2406-2412.
[37] B. Theisen, E. Zeiske, H. Breucker, Functional morphology of the olfactory organs in the spiny dogfish (Squalus acanthias L.) and the small-spotted catshark (Scyliorhinus canicula (L.)), Acta Zool. 67 (1986) 73-86.
[38] P.M.S. Monk, Fundamentals of electroanalytical chemistry, Wiley, New York, 2001.
[39] C. Iliescu, H. Taylor, M. Avram, J.M. Miao, S. Franssila, A practical guide for the fabrication of microfluidic devices using glass and silicon, Biomicrofluidics 6 (2012) 016505.
[40] Y.J. Chuang, F.G. Tseng, W.K. Lin, Reduction of diffraction effect of UV exposure on SU-8 negative thick photoresist by air gap elimination, Microsyst. Technol. 8 (2002) 308-313.
[41] R.A. Lawes, Manufacturing tolerances for UV LIGA using SU-8 resist, J. Micromech. Microeng. 15 (2005) 2198-2203.
[42] K.C. Honeychurch, S. Al-Berezanchi, J.P. Hart, The voltammetric behaviour of lead at a microband screen-printed carbon electrode and its determination in acetate leachates from glazed ceramic plates, Talanta 84 (2011) 717-723.
[43] L.C.S. Figueiredo-Filho, B.C. Janegitz, O. Fatibelilo-Filho, L.H. Marcolino-Junior, C.E. Banks, Inexpensive and disposable copper mini-sensor modified with bismuth for lead and cadmium determination using square-wave anodic stripping voltammetry, Anal. Methods 5 (2013) 202-207.